

NUMERICAL STUDY OF CAVITATING FLOW IN ASYMMETRICAL NOZZLES OF INJECTORS/ATOMIZERS. PART I. ASSESSMENT OF CALIBRATED EDDY VISCOSITY MODELS IN DEVELOPING CAVITATION CASES

Miguel G. Coussirat, Flavio H. Moll

*Laboratorio de Modelado Aeroelasticidad (LaMA), Universidad Tecnológica Nacional (UTN),
Facultad Regional Mendoza (FRM), Argentina, miguel.coussirat@frm.utn.edu.ar,
flavio.moll@docentes.frm.utn.edu.ar <http://www.frm.utn.edu.ar>*

Keywords: Developed Cavitation; Injectors; Atomizers; Turbulence; Eddy Viscosity Models; Validation/Calibration.

Abstract: Cavitating flow is related to turbulent and multiphase flows with mass transfer between the liquid and its gaseous phase. Cavitation in pressure injectors/atomizers strongly affects the liquid/spray jet behavior at its outlet. The type of atomization induced by cavitation allows developing more efficient devices if this cavitation state is controlled. Experiments show that an improvement in the quality of the spray is reached when a fully developed cavitation state is present at the nozzle, being this state clearly unsteady due to the presence of the re-entrant jet and the vortex shedding downstream of the cavity. Previous works showed that it is possible to capture several of the incipient cavitating or quasi-steady cavitating flow characteristics performing a careful calibration of the available Eddy Viscosity Models in nozzles with several inlet and outlet geometries. A careful calibration of the selected Eddy Viscosity Model becomes an important task to obtain accurate predictions of the flow both in quasi-steady and unsteady cavitation states. The numerical results discussed in this first part show that it is possible to capture the main cavity features by a steady state cavitation simulation despite the incipient unsteady state of the slightly developed cavitation state. It is demonstrated that the obtained results become competitive when they are compared against ones computed by Large Eddy Simulations which need a lot of computational resources and an appropriate initial solution for running. The possibility to perform unsteady simulations using Eddy Viscosity Models is explored. As a first step, a discussion of the experimental data available for fully developed cavitation cases and the developed simulation strategies to carry out these cases are presented.

1. INTRODUCTION

In liquid flows, cavitation generally occurs if the pressure in certain locations drops below the vapor pressure. These low pressures provoke the emerging cavities apparition filled with gas and vapor. This phenomenon can be observed in a wide variety of hydraulic devices, and it is well known that this kind of two-phase flow is usually related with a lot of unpleasant results (Zhang et al., 2011). More in detail, cavitation appears in liquid flows when the local hydrodynamic pressure, p_c in some place falls reaching the vapor pressure of the liquid, p_v . This low-pressure level provokes that the initial liquid flow becomes a two-phase flow, i.e., liquid-bubbles of vapor. The initiation of cavitation by liquid vaporization may require the existence of stresses lower than vapor pressure due to the surface stress tension in the bubble. However, the presence of undissolved gas particles, boundary layers, and turbulence will modify and often mask a departure of this critical pressure p_c from p_v , (Coussirat et al., 2016).

Because studies by physical experiments are very expensive (high-speed flow and small spatial and time scales involved), Computational Fluid Dynamics (CFD) codes, based on a certain kind of ‘multiphase flow modeling’ technique have been specifically adapted/developed for studying cavitating flows, involving both turbulence and mass transfer modeling. Thus, a Reynolds Averaged Simulations (i.e., steady RAS, or transient/unsteady URAS) plus Eddy Viscosity formulations, RAS/URAS+EVMs, for the mixture (liquid+vapor) joined to a Transport Equation-based Modeling, TEM, are used. The CFD models based in RAS/URAS+EVMs is now a common option for numerical simulations of turbulent flows. For cavitating flow modelling, the TEM technique consists in solving a transport equation for either mass or volume fraction with appropriate source terms to regulate the mass transfer between phases. Therefore, RAS/URAS+EVMs+TEM constitutes the complete model for cavitating flows, (see full details in Coussirat et al., 2016-2021).

Specifically, in fuel injectors for Diesel engines, the occurrence of cavitation inside an injector nozzle is also directly connected with the local pressure drop. Understanding the cavitating flow phenomenon in fuel injector nozzles has major importance, since it plays a significant role in the spray atomization at its outlet, affecting Diesel engines performance and emissions. The type of atomization induced by cavitation allows developing efficient devices if this cavitation state is controlled. By means of numerical simulations using uncalibrated EVMs, some of the incipient and slightly developed cavitating flow characteristics in nozzles could be captured by steady state simulations, but the vapor fraction level in the cavities, vf , is commonly underestimated, (Coussirat et al., 2016).

This work is related to cavitating flows CFD modeling in low pressure Diesel injectors with an asymmetrical nozzle inlet configuration and square sections at the outlet, under transient state cavitating flow conditions, (i.e., slightly developed cavitation and fully developed cavitation states), see Fig. 1. The main subject here is to obtain a better performance of RAS/URAS+EVMs developed for general usage when they are applied to design devices where cavitating flows appear. Previous works showed that a careful EVM calibration is necessary, and it must rely on a physical basis. Conclusions obtained from Coussirat et al., 2016-2021 for steady cavitating flow simulations are a useful tool for performing succeeding URAS+EVMs simulations.

2. EXPERIMENTAL DATABASES USED

For URAS/EVMs CFD some of the experiments used in the quoted works were revisited, e.g., Sou et al., 2014, and Biçer 2015, because a detailed cavity dynamic and measurements of the velocity and turbulence fields were given. The experimental setup consists in the use of a plunger pump to discharge filtered tap water at an ambient temperature (19°C) into ambient air through a rectangular nozzle, Fig. 1. The width of the upstream region (injector inlet) is four times wider than the nozzle width. The liquid flow rate was measured using a flowmeter inserted

in the hydraulic circuit. The static pressure upstream of the nozzle was measured, but the exact position of this pressure probe (gauge pressure) was not clearly defined. Both the mean velocity, c_m and its RMS fluctuation c'_{RMS} , (y direction) were measured by a Laser Doppler Velocimeter, LDV, system under slightly developed cavitation conditions. The measurements were taken on the middle plane in depth of the nozzle channel at three positions (y_1, y_2, y_3) referred to the defined nozzle coordinate system, marked on the Fig. 1.

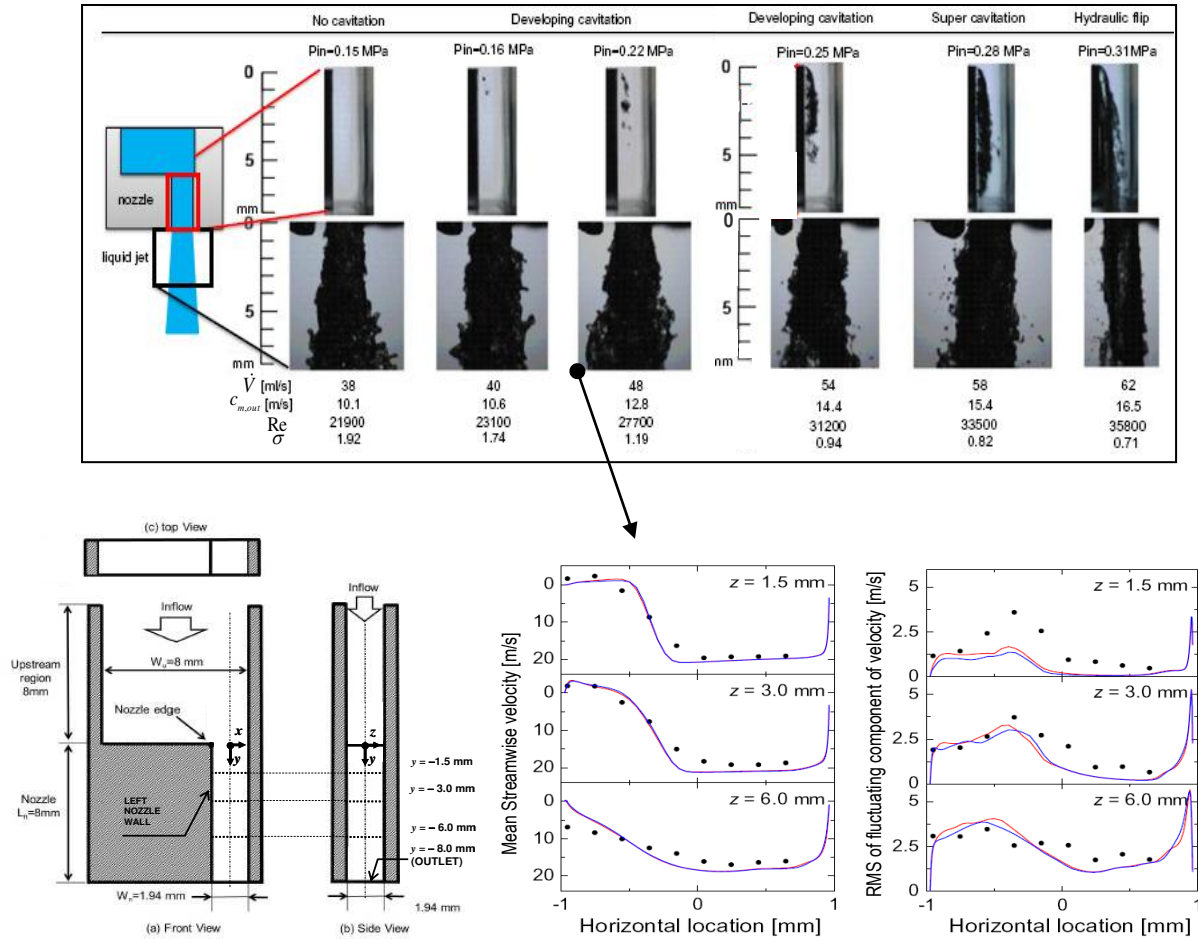


Figure 1. Geometry, experimental and CFD mean c_m and RMS fluctuating c'_{RMS} velocity profiles, for Reynolds number, $Re = 27,700$. Notation: σ , K, Cavitation numbers; Re, Reynolds number, see Eq. 1. •, Experiments (LDV); CFD Smagorinsky (Red) and Vreman (Blue) LES SGS models respectively, Sou et al., 2014 and Biçer 2015. Equivalence (σ , K): (1.92, 3,00); (1.19, 1,83); (0.94, 1,66)

The measurements uncertainty reported were $\sim 1\%$ and $\sim 3.7\%$ for LDV and flow rate respectively. Commonly, the showed cavitation states from Fig. 1 are classified by a two characteristic numbers, i.e., Reynolds, Re, and Cavitation, σ , K, numbers, see Eq. 1:

$$\begin{aligned} Re &= c_{m,out} w_n / \nu; \quad We = \rho c_{m,out}^2 th_n / \tau_s; \quad Sr = f_{vs} L_{cav} / c_{m,out} \\ \sigma &= (p_{out} - p_v) / (0.5 \rho c_{m,out}^2); \quad K = (p_{out} - p_v) / (p_{in} - p_{out}); \end{aligned} \quad (1)$$

Being We and Sr, the Weber and Strouhal number respectively; w_n, L_n, th_n , nozzle width, length and thickness respectively; $c_{m,out}$, outlet mean velocity; f_{vs} , vortex shedding frequency; ν , liquid viscosity ($=1.035 \times 10^{-6} \text{ m}^2/\text{s}$); ρ , liquid density ($=998 \text{ kg/m}^3$); p_{in} , inlet pressure; τ_s , surface stress ($=7.28 \times 10^2 \text{ N/m}$); p_{out} , outlet pressure ($=1.0 \times 10^5 \text{ Pa}$); p_v , vapor pressure ($=2,300 \text{ Pa}$); L_{cav} ,

cavity mean length. Depending on the σ value, there are several stages in the developing cavitation state before to reach the supercavitation state. A quasi-state stage ($\sigma=1.74$) without vortex shedding and an incipient unsteady stage that shows some vortex shedding evidence ($\sigma=1.19$) can be observed.

It is highlighted that: 1) Re and σ (or K) numbers are not closely related (Coussirat et al., 2021), being both necessary for the cavitating state identification. 2) The two commonly used cavitation number definition (σ and K) were given because different authors present results from experiments using one or other. Unfortunately, no information related to the injection pressure to compute these numbers was given. Therefore, the equivalences between σ and K are only indicative of a possible similar cavitation state here, being not rigorous because comparisons for the same cavitation state in slightly different geometries, e.g., Sou et al, 2014, Biçer 2015, give different σ and K values. The different cavitation states were generated changing the flow rate (or the p_{in}), because the p_{out} remains constant, having a free jet flow at the outlet (i.e., subsonic flow with negligible surface stresses).

The We is an important nondimensional parameter in liquid atomization and related to the importance of the surface stresses. It was computed to check their influence in the studied cases, Eq. 1. The We obtained was of O(10), meaning that under these conditions the inertial forces are almost ten times stronger than the surface forces justifying the assumption of negligible surface effects under these cavitation states, (Coussirat et al., 2021).

Several attempts were made to characterize the v_f in the cavity. Barre et al., 2009 carried out some v_f measurements in Venturis for stable cavities reporting a strong v_f variability in the cavity that prevents to obtain a mean value estimation of the v_f . Experiments from Sou et al, 2014 and Biçer 2015 showed some representative images for the ‘mean’ transient cavity obtained for each cavitation state in nozzles, see Fig. 1, but neither the v_f nor the local pressure in the cavity were measured. It was demonstrated that under strong decrements in the σ values, the vortices appear clearly, and they are advected downstream with certain characteristic shedding frequencies. These vortices are also accompanied by clouds of vapor bubbles that collapse during the shedding when the pressure rises downstream again. It can be observed that this transition from steady to transient states is quite snappish, probably due to the short length of the nozzle in this case (i.e., a ratio $L_n/w_n < 5$), being this fact an added difficulty for the CFD modeling, (Coussirat et al., 2016-2021).

2.1. Interaction between turbulence and cavitation

Cavitation always involves complex interactions between turbulent flow structures and multiphase dynamics in internal and external flows, (Singhal et al., 2002, Korkut et al., 2002, Sou et al, 2014). The viscous nature of the flow, particularly the free-stream turbulence, is one of the main factors contributing to the scale effects on the inception of cavitation. It is known that a high turbulence level (i.e., level of turbulent kinetic energy, k) causes an early transition to turbulence in the boundary layer, which, in turn, can lead to the complete elimination of the laminar separation. In this context, it was demonstrated that the viscous effects associated with the laminar separation and transition of the boundary layer have a major effect on the cavitation inception. The involved k level influences the inception of cavitation when it can cause significant change in transition and/or laminar separation.

It was also demonstrated that the k level in the free-stream zone could be responsible for different results for the cavitation inception of identical bodies tested in different facilities, (Korkut et al., 2002). The increase in the k level shifted the laminar separation point forward and, hence, enforced the boundary layer to become almost fully turbulent. This will have a twofold effect on cavitation inception: 1) The structure of the cavities will be altered, i.e., the cavity

shape and its dynamics are strongly dependent on the Re . 2) It will allow for early transition to turbulence, which, in turn, will show its effect on the inception and developing cavitation phenomena.

From the CFD viewpoint, Coussirat et al., 2021, reported that for states of incipient cavitation, the obtained results have a higher dependence on the EVMs than on the TEMs selected in cases of low-pressure Diesel injectors. The TEMs checked have shown slight differences in the cavity shape and its νf level predicted. It was demonstrated that it is possible to capture several of the incipient cavitating flow characteristics by means of a careful EVM calibration due to the close relation between the cavitation state and the k level in the flow. This could both related to the spatial distribution of k and its decay rate computed, leading to some preferred turbulence scales under the cavitation process, and provoking a ‘non-standard turbulence state’ as experiments show. So, cavitating flows should not be modeled like a simple (or ‘classical’) shear turbulent flow. Uncalibrated EVMs overpredict the level of the eddy viscosity, μ_t , and compute lower dynamic pressure levels, yielding a higher static pressure and less νf , affecting directly the cavity shape due to the high stresses computed, and limiting both pressure and velocity predictions in the recirculation zones, (Shi et al., 2010, Biçer 2015, Coussirat 2016).

2.2. Developed cavitation: turbulence and unsteadiness

When the state of the cavitation migrates from incipient, i.e., $\sigma = 1.74$, to slightly developed, i.e., $\sigma = 1.19$, a series of phenomena related to the flow unsteadiness appears, (Wang et al., 2018, Stanley et al., 2011, Stanley et al., 2014, Sou et al., 2014, Biçer 2015). An important phenomenon in the process is the motion of a liquid jet beneath the fixed cavity in the direction counter to the main flow, referred to as the ‘re-entrant’ jet. The mechanism which drives this phenomenon remains unclear, particularly for cavitation in nozzles because there are not so many studies for this phenomenon in orifice atomizers, (Stanley et al., 2014). Typically, it is observed that it is created by the flow expanding in the closure region behind the cavity, impinging against the wall and establishing a local stagnation point. On the upstream side of the stagnation point conservation of momentum forces the fluid to flow beneath the fixed cavity. The jet progresses and when it reaches the vicinity of the leading edge it ‘pinches-off’ the fixed cavity allowing it to be shed and form a vapor cloud. As the cloud is shed a new fixed cavity forms at the leading edge and begins to grow. As the separated cloud is advected downstream it coalesces and forms a rolling vortex due to the momentum of the free stream.

Due to this cyclic nature the cavity periodic shedding is a common form of cavitation instability. An important parameter to account for this unsteadiness is the vortex/cavity shedding frequency, f_{vs} . Experiments from Biçer 2015, reported shedding and collapse cavitation clouds frequencies values in a range of 1 - 4 kHz in a square section nozzle with a symmetrical inlet and for a mean inlet velocity, $c_{m,in} = 17.5$ m/s ($\sigma = 0.65$, $Re = 6.9 \times 10^4$). Stanley et al., 2011 reported that in a circular nozzle of $D = 8.25$ mm and for values of $K = 1.85$ cavitation occupied less than 30 % of the nozzle length, exhibiting a periodic bubble cloud shedding, with a fundamental frequency (f_{vs} first mode) between 0.5 and 2.0 kHz. Experiments on a water cavitating orifice with $D=2.5$ mm were conducted to investigate the influence of pressure and temperature on the flow regime transition due to cavitation by De Giorgi et al 2013. The nozzle operating conditions were: $3.8 \times 10^4 < Re < 18.9 \times 10^4$; $4.11 > K > 1.34$ and $T = 293$ K. Measurements in two positions along the nozzle showed a dominant f_{vs} in the 0.15 - 0.3 kHz range. At higher K , a fixed cavity took place at the inlet of the orifice and an unsteady shedding behavior was present in the vapor structures. Sato et al., 2002 present results in orifices ($15 \text{ mm} < D < 22 \text{ mm}$) with different nozzle length ($50 \text{ mm} < L_n < 100 \text{ mm}$) and under different flow conditions ($1.66 \times 10^5 < Re < 2.38 \times 10^5$; $0.97 > K > 0.83$). The f_{vs} first mode found was of 0.25 - 0.35 kHz and they also

reporting that in the exit area it was possible to identify at least three different f_{vs} components: one in the 0.03 - 0.06 kHz range, the second in the 0.2 - 0.3 kHz range and the last in the 0.75 - 0.90 kHz range. Compilation of the f_{vs} first mode observed reveals a linear trend of increasing frequency with increasing K (or σ) values. A similar order value (0.9 kHz) for the f_{vs} first mode was measured in a $D = 8.25$ mm nozzle by [Stanley et al., 2014](#) for defined $K = 1.80$ and $Re = 6.9 \times 10^4$ values ($c_{m,out}$ of 12.82 m/s).

On the other hand, a CFD investigation of the re-entrant jet dynamics in a cavitating nozzle flow by means Large Eddy Simulations, LES was performed by [Trummler, 2020](#) reporting a f_{vs} first mode of 1.110 kHz for the [Sou et al, 2014](#) case ($\sigma=1.19$, $Re = 2.7 \times 10^4$).

3. METHODOLOGY DEVELOPED FOR RAS/URAS+EVM/TEM MODELING

The EVM calibration is as important as the derivation of the model itself. Calibration is achieved with the help of experimental and validated CFD results of the flow that should be modeled. The calibration process is also the first step in which the range of validity of the model would be checked by a detailed inspection and not just by its initial physical model definition. The previous works for RAS/EVMs calibration were related to no cavitating and incipient cavitating flows in nozzles, i.e., steady state cases, ([Coussirat et al., 2016-2021](#)). The studies consisted in EVMs and TEMs calibrations by means of a careful parameters selection/tuning, joined to a mesh sensitivity study. The parameters selection must be performed considering the close relation between the cavitation state and the k level in the flow considering the characteristics of detached flows. The followed methodology to guarantee accurate results included: 1) A study of the grid independence of the results by the Grid Convergence Index method, GCI, and the Richardson extrapolation technique. 2) A detailed EVMs calibration using the experimental database from [Biçer 2015](#). 3) A careful performance comparison among several TEMs models, see details in [Coussirat et al., 2016-2021](#).

The main conclusion obtained was that it is more important a detailed calibration study for the EVMs models than for the TEMs ones. The depicted methodology could be a good general strategy in the sense that it has been defined by physical reasoning related to the differences in the flow structure between simple shear and detached flows. A summary of the results obtained, and the main conclusions related to the use of steady state CFD simulations for the developing cavitation case is presented in the next section.

4. INCIPIENT CAVITATION STATE SIMULATIONS BY MEANS OF RAS/EVM

A steady state simulation of the nozzle was performed to reproduce the cavity behavior under these conditions (i.e., $\sigma = 1.91$, $\sigma = 1.19$, see full details in [Coussirat et al., 2016-2021](#)). Conclusions of these works allow to select the SST $k-\omega$ model (SST) from [Menter 1994](#), and [Menter et al, 2003](#) for turbulence modelling and the [Singhal et al., 2002](#) model for cavitation for the present study; remarking that it is more important the EVM calibration than the TEM ones. Specifically for the SST model, the parameter β^*_∞ was selected for calibration, since it is responsible for the computed level in the dissipation of k , and the production of ω in the model equations. This parameter also controls the boundary conditions computed for k and ω at the walls. The base value for β^*_∞ (=0.09) has been established by examining the so-called ‘wall layer’ ([Wilcox, 1988](#)). The reason is the following: In boundary layer flows the wall layer is defined as the portion of the boundary layer far enough from the surface to render molecular viscosity negligible relative to the turbulent viscosity of the mixture (liquid+vapor), $\mu_{t,m}$, but close enough for convective effects to be negligible relative to the rate at which the turbulence is being created and destroyed (equilibrium turbulence state). Notice that the Reynolds shear stress τ is constant in the wall layer and equal to the friction velocity (or shear velocity, u_τ) implying

that $\tau/k = \sqrt{\beta_\infty^*}$ and leading to the standard value for β_∞^* , because a variety of experimental measurements indicate that for simple shear flows the ratio of τ/k is about 3/10 in the wall layer (Townsend, 1976). Thus, the predicted wall layer solution is consistent with experimental observations, providing this base value for β_∞^* for simple shear flows.

After this analysis of the SST model ‘structure’ and the parameters selection for calibration, a commercial CFD code (Ansys, 2018) was used to simulate an incipient cavitation state, (i.e., $\sigma = 1.19$, see Fig.1) with a fine tuning of the parameter β_∞^* . A two-dimensional (2D) structured 50,000 cells mesh was defined after the GCI and the Richardson extrapolation (mesh M03, cell area of $h \times h$, $h = 0.004$ mm, see details in Coussirat et al., 2021) over the nozzle geometry, Fig. 1. The grid sensitivity study and comparison between 2D and 3D ($\sim 50 \times 10^6$ cells) simulations already performed in Coussirat et al., 2021 allows ensuring both independence of the obtained results to the defined cell size and negligible 3D effects in the flow over its middle plane. The inlet boundary condition was defined as a mean value for the mean velocity at the inlet $c_{m,in}$ which was computed from the mass conservation principle, because the inlet/outlet geometry sections and the mean velocity at the outlet, $c_{m,out} = f(\sigma)$ are known in advance. At the outlet, a static pressure value was imposed ($p_{out} = 1.0 \times 10^5$ Pa) and a non-slip condition was defined at the walls. The turbulence inlet/outlet boundary conditions were computed from standard formulations for the turbulent kinetic energy, k , and its dissipation, ω . The selected discretization schemes were: QUICK, for ρ and vf ; Least Squares Cell based, for the Gradients in the spatial discretization; Bounded Central Differencing, for the momentum discretization; PRESTO, for pressure and SIMPLEC, for pressure-velocity coupling (Versteeg et al., 2007, Ansys 2018).

After each CFD modeling, the predicted inlet pressure p_{in} and its corresponding σ (or K) value was computed and then, verified for each case. Comparisons between experiments and CFD simulations were performed for: 1) The averaged mean velocity at the outlet i.e., $c_{m,out}$, Table. 1. 2) Both c_m and c'_{RMS} profiles at positions y_1 , y_2 and y_3 , Fig. 2. 3) The cavity shape in terms of its vf contours (see the discussion in the second part of this work).

Exp.	SST ($\beta_\infty^* = 0.09$, default)	SST ($\beta_\infty^* = 0.11$)	SST ($\beta_\infty^* = 0.18$)
12.800	12.724	12.734	12.790
Error (%)	0.59	0.51	0.08

Table 1. CFD results: Mean velocity averaged at the outlet, $c_{m,out}$, [m/s]. The error was computed taking as the exact value the measured one.

Table. 1 shows that the SST model underpredict the $c_{m,out}$ when the default calibration value was used. Under the fine tuning of β_∞^* , it was observed that the $c_{m,out}$ predictions are improved. In order to check if calibration allows saving some CPU resources, comparisons were carried out against: 1) The results from Biçer 2015 computed by using selectively refined grids ($\sim 7.3 \times 10^4 - 6.2 \times 10^5$ cells) using the RNG and SST models, Fig. 2. 2) The results from Sou et al, 2014 and Biçer 2015 computed by using the LES Smagorinsky and Vreman’s SGS models, see Fig. 1 and Fig. 2. These LES results needed time steps of order $O(10^{-8}s)$, about 7.0×10^5 cells for a precursor simulation to obtain a suitable inlet boundary condition and 2.8×10^6 cells in the nozzle simulations involving a Linux computer with 3.0 GHz \times 32 core, 16 CPU and 64GB/RAM node. The CPU time for a precursor simulation was about three weeks to reach a steady state, while that for a nozzle simulation was about one week (Sou et al, 2014, Biçer 2015).

Fig. 2 shows that the SST model gives quite good predictions for the c_m profiles at all the checked positions. The comparison against LES results from Fig.1 shows a similar quality for the c_m adjustments obtained here (not shown here, see details in Coussirat et al., 2021). On the other hand, the results obtained for the c'_{RMS} profiles have similar quality as the adjusts obtained

by uncalibrated EVM but with finer meshes from Biçer 2015, or ones obtained by Sou et al, 2014 and Biçer 2015 using LES over very refined meshes.

It is shown that depending on the selected value for β^*_{∞} , the μ_t is suppressed at position y_I leading to a rise in the vapor fraction predicted. Therefore, the incipient/developed unsteady nature of cavitation at $\sigma = 1.19$ in this geometry is captured despite the steady state simulation performed, because: 1) The ‘incipient shedding’ is better observed. 2) The $c_{m,out}$ prediction improves, see Table 1. 3) The fluctuating velocity field, c'_{RMS} , at the nozzle inlet it is better adjusted for $\beta^*_{\infty} > 0.09$ values, Fig. 2.

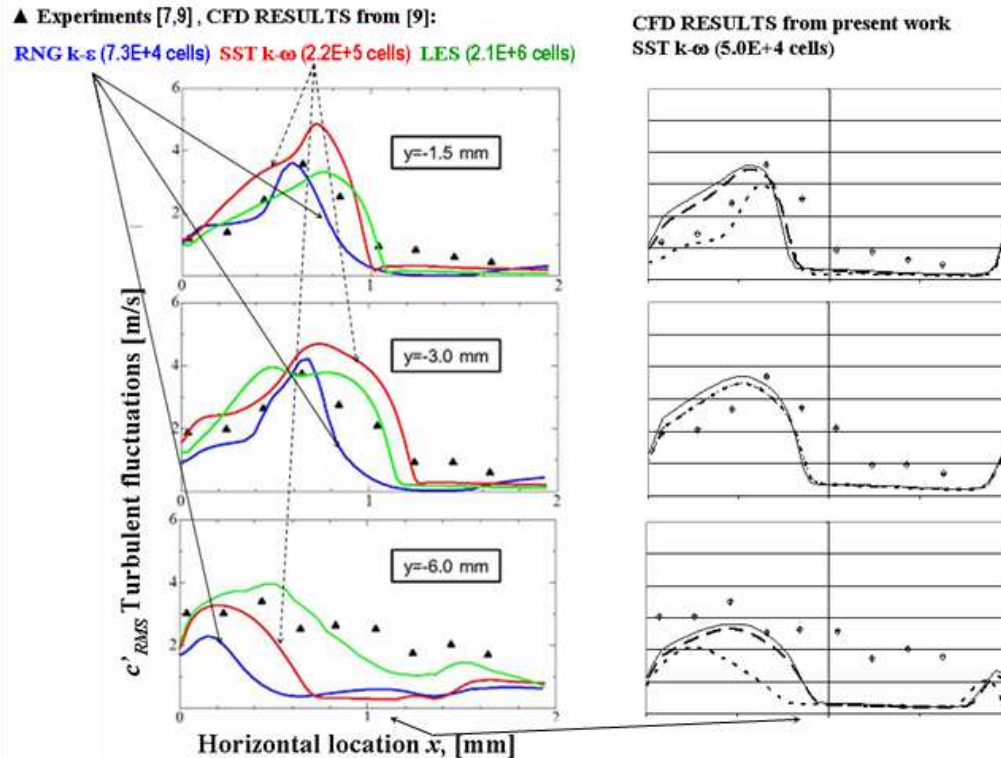


Figure 2 : CFD results (M03, $\sigma = 1.19$, β^*_{∞} sensitivity study): Fluctuating velocity profiles: c'_{RMS} . **Left:** CFD results extracted from Ref.[9]. **Right** CFD present work: **Nomenclature:** \circ , \blacktriangle Experimental results from Refs. [7,9], (vertical bars point out uncertainty in the right graphic); CFD: —, 0.09; - - -, 0.12; ----, 0.18.

Unfortunately, in the experiments from Sou et al, 2014 and Biçer 2015 there is no quantitative information about the νf level and in the CFD simulations there are no images with the cavity shape for $\sigma = 1.19$. Therefore, only the cavity shape from experiments could be compared against the present CFD results, assuming that in the cavity shown by the experiments the νf levels are not nearer the unity, since the fluid reached the incipient cavitation state only. These results will be presented in the second part of this work.

5. CONCLUSIONS

The methodology for the calibration performed in previous works has been validated and could be a good general strategy in the sense that it was defined in terms of physical reasoning related to the differences in the flow structure when shear flows and detached flows are compared.

The improvements in the obtained results are justified in the fact that for the SST model the coefficient β^*_{∞} is responsible for the computed k and ω levels. Therefore, the main characteristic

of the geometry (i.e., the step in the nozzle) is related to the k production, not to the k dissipation, being the last effectively related to β^* .

At $\sigma = 1.19$ a steady state simulation is still possible to compare experimental data and CFD results for both mean and fluctuating velocity fields. It is demonstrated that the improvements in the fluctuating velocity field, c_{RMS} , predictions provoke a more accurate cavity shape prediction. The mean velocity field cm does not suffer strong variations when the calibration is performed, but the c_{RMS} field predicted is strongly affected by the calibration. This fact remarks the close relation between the turbulence level and the cavitation inception phenomenon because it was demonstrated that suppressing the $\mu_{t,m}$ level by calibration, the vf predicted rises.

The promising SST model performance led to its applications to unsteady turbulence modeling in the second part of this work. Both the SST and SST/SAS models (Egorov et al., 2010 and Menter et al., 2010) would allow studies of developed cavitating flows by means of an unsteady less expensive URAS simulation than the LES one. URAS simulations still could be competitive for unsteady/transient state simulations if a careful compromise between very detailed results and CPU requirements is considered.

ACKNOWLEDGEMENTS

This current work was partially supported by the Universidad Tecnológica Nacional (UTN) within its own research programme (UTN/SCTyP). Authors would like to express their appreciation to the UTN for providing financial support for this study (research project UTI4905TC).

REFERENCES

- Ali M., Doolan C., Wheatley V., Convergence Study for a Two-Dimensional Simulation of Flow Around a Square Cylinder at a Low Reynolds Number, *7th Int.Conf. on CFD in the Minerals and Proc.Industr. CSIRO*, Australia, 2009.
- Ansys/Fluent Software, 2020, <http://www.ansys.com/Industries/Academic/Tools/v15Tutorial>.
- Barre, S., Rolland, J., Boitel, G., Goncalves, E., and Patella, R., Experiments and modeling of cavitating flows in venturi: attached sheet cavitation. *Europ. J. of Mechanics-B/Fluids*, 28(3), pp444-464, 2009.
- Biçer B., Num. Simul. of Cavitation Phenomena inside Fuel Injector Nozzles, *PhD Thesis, Kobe Univ. Japan*, 2015.
- Coussirat, M., Moll, F., Cappa, F., and Fontanals A., Study of Available Turbulence and Cavitation Models to Reproduce Flow Patterns in Confined Flows,” *J. Fluids Eng.*, 138(9), 2016.
- Coussirat M., Moll F. and Fontanals A., Reproduction of the cavitating flows patterns in several nozzle geometries using calibrated turbulence and cavitation models, *Mec. Computac.*, Vol XXXV:819–841, 2017.
- Coussirat, M., Moll, F., Recalibration of Eddy Viscosity Models for Numerical Simulation of Cavitating Flow Patterns in Low Pressure Nozzle Injectors. *J. of Fluids Engineering*, 143(3), 031503, 2021.
- De Giorgi, M. G., Ficarella A., and Tarantino M., Evaluating cavitation regimes in an internal orifice at different temperatures using frequency analysis and visualization. *Int.J. Heat and Fluid Flow* 39, pp160-172, 2013.
- Egorov, Y., Menter, F., Lechner, R., and Cokljat, D., The Scale-Adaptive Simulation Method for Unsteady Turbulent Flow Predictions—Part 2: Application to Complex Flows, *Flow Turb. Combust.*, 85(1), pp.139–165, 2010.
- Korkut E. and Atlar M., On the importance of the effect of turbulence in cavitation inception tests of marine propellers, *Proc. R. Soc. Lond. A*, 458, pp29-48, 2002.

- Menter F., 'Two Equations Eddy-Viscosity Turb. Models for Eng. Appl.', *AIAA J.*, 32(8), pp. 1598–1605, 1994.
- Menter, F., and Egorov, Y., 'The Scale-Adaptive Simulation Method for Unsteady Turbulent Flow Predictions—Part 1: Theory and Model Description,' *Flow Turb. Combust.*, 85(1), pp. 113–138, 2010.
- Menter, F., Kuntz, M., and Langtry, R., 'Ten Years of Industrial Experience With the SST Turbulence Model,' *Turb., Heat and Mass Transfer*, Vol.4, K. Hanjalic, et al., eds., House, pp. 625–630, 2003.
- Sato, K., Saito, Y., Unstable cavitation behavior in a circular-cylindrical orifice flow. *JSME Int.J. Series B Fluids and Thermal Engineering*, 45(3), pp638-645, 2002.
- Shi J. and Arafin M., CFD investigation of fuel property effect on cavitating flow in generic nozzle geometries, *ILASS–Europe2010, 23rd Ann. Conf. on Liquid Atomiz. and Spray Syst.*, Czech Republic, 2010.
- Sou A., Biçer B., Tomiyama A., Num. simulation of incipient cavitating flow in a nozzle of fuel injector, *Comp&Fluids* 103: pp42–48, 2014.
- Singhal, A., Athavale, M., Li, H., and Jiang, Y., Math. Basis and Validation of Full Cavitation Model, *J. Fluids Eng.* 124(3): pp617–624, 2002.
- Stanley, C., Barber, T., Milton, B., & Rosengarten, G., Periodic cavitation shedding in a cylindrical orifice. *Exp. in fluids*, 51(5), pp1189-1200, 2011.
- Stanley, C., Barber, T. and Rosengarten, G., Re-Entrant Jet Mechanism for Periodic Cavitation Shedding in a Cylindrical Orifice. *Int J. Heat and Fluid Flow*, 50, pp169-176, 2014.
- Trummler T., Num. investig. cavitation phenomena, *PhD Thesis, Technische Universität München*, Germany, 2020.
- Townsend, A., 'The Structure of Turbulent Shear Flow', 2nd ed., *Cambridge University Press, Cambridge, England*, pp. 107-108, 1976.
- Versteeg H. and Malalasekera W., 2007, 'An Introduction to Computational Fluid Dynamics: The Finite Volume Method,' 2nd Ed., *Upper Saddle River, NJ, USA*, Pearson Prentice Hall; 2007.
- Wang Z., Zhang M., Kong D., Huang B., Wang G., Wang C., The influence of ventilated cavitation on vortex shedding behind a bluff body, *Exp. Therm Fluid Sci.*, 98, pp181-194, 2018.
- Wilcox D., 'Reassessment of the Scale-Determining Equation for Advanced Turbulence Models,' *AIAA Journal* 26(11), 1988.
- Zhang, J. M., Qing, Y. A. N. G., Wang, Y. R., Xu, W. L., & Chen, J. G. Experimental investigation of cavitation in a sudden expansion pipe. *Journal of Hydrodynamics, Ser. B*, 23(3), 348-352, 2011.